Cu^{2+}-selective naked-eye and fluorescent probe: its crystal structure and application in bioimaging†

Fabiao Yu, Wenshen Zhang, Ping Li, Yanlong Xing, Lili Tong, Jianping Ma and Bo Tang*

Received 14th January 2009, Accepted 2nd July 2009
First published as an Advance Article on the web 17th July 2009
DOI: 10.1039/b823360h

A new fluorescent and colorimetric Cu^{2+} probe was synthesized, and realized optical imaging in RAW264.7 macrophages. The design strategy was based on a change in structure between spirocyclic (non-fluorescent) and ring-open (fluorescent) forms of rhodamine-based dyes, and its crystal structure was presented to explain the binding mode. Upon treatment with Cu^{2+}, the weakly fluorescent probe exhibited a strong fluorescence response, high selectivity and was quantitative for Cu^{2+} under physiological conditions. In addition, the off–on-type fluorescent change upon the addition of Cu^{2+} was also applied in bioimaging.

Introduction

Copper is the third-most abundant transition metal in the body.[1] The redox-active nutrient is needed at unusually high bodily levels for normal physiological functions. Cu^{2+} plays a critical role as a catalytic cofactor for a variety of metalloenzymes and transcriptional events,[2,3] and the transition metal ion also holds responsibility for physiological responses to stress and panic, as well as for dopamine production.[4] An alteration of intracellular copper ion homeostasis is connected to various neurodegenerative diseases, including Menkes and Wilson's diseases,[5–7] familial amyotrophic lateral sclerosis,[8,9] Alzheimer's disease,[10] and prion disease.[11] However, with excessive loading, Cu^{2+} is highly toxic to organisms.[12] All of these events above demonstrate that the quantitative detection of intracellular Cu^{2+} is of great importance for elucidating the complex physiological and pathological roles of copper.

In recent years, the fluorescence method of detecting metal ions has attracted great attention, mainly due to its distinct advantages in sensitivity, selectivity and on-line imaging. As far as we know, many fluorescent probes have greatly facilitated the study of diamagnetic metal ions, such as Pb^{2+}, Hg^{2+}, Zn^{2+}, and Cu^{+}.[13–21] However, for Cu^{2+}, its intrinsic fluorescence quenching property inhibits the development of the fluorescent probe for Cu^{2+}. Most Cu^{2+} probes show a 'turn-off' (fluorescence quenching) response[22–33] *via* an energy or electron-transfer process.[34,35] Among the reported 'turn-on'-type Cu^{2+} probes,[36–45] few have nanomolar sensitivity,[36,39,41,42,45] and high selectivity.[36,39,45] Recently, a copper probe has been reported.[46] The probe has been applied *in vivo*, but quantitative detection of Cu^{2+} under physiological conditions is not involved much. Here, we describe an example of Cu^{2+}-selective probe, which is suitable for quantitative detection of Cu^{2+} under physiological conditions. Furthermore, the probe displays a dependent fluorescence response to varying levels of intracellular copper ions.

Rhodamine-based dyes, which are excited by visible light, exhibit turn-on response to many targeted cations, such as Pb^{2+},[47] Hg^{2+},[48–53] Fe^{3+},[54] and Cu^{2+}.[55] However, the fluorescent probes reported above are mostly used in organic solvents for the detection of metal ions,[47–49,51,55] which makes them difficult to be applied in biological system. Besides, the interference experiments of these methods only achieve equivalent coexistence of interference substances with Cu^{2+}, which are not suitable for detecting in complex biological environments.

Herein, we designed and synthesized a new fluorescent probe **2** (Scheme 1) to detect Cu^{2+}, with rhodamine 6 G as the fluorophore and 2-acetyl-(1,4)-benzodiazine, a Cu^{2+}-selective ligand, as the ion acceptor. The weakly fluorescent probe showed a fluorescence enhancement response upon binding with Cu^{2+}. The coexistence experiment demonstrated that probe **2** has a high selectivity to Cu^{2+} while present with high concentrations of other biologically relevant metal ions, such as Na^{+}, K^{+}, Ca^{2+}, Mg^{2+}, and Zn^{2+} (1000 equivalent tolerance), and other first-row

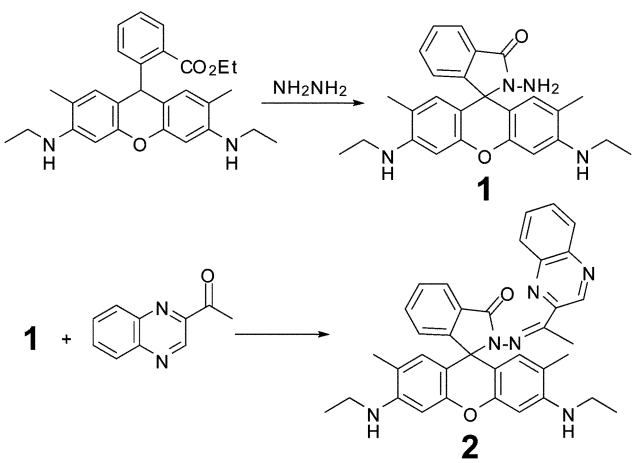

Scheme 1 Synthesis of **2**.

College of Chemistry, Chemical Engineering and Materials Science, Engineering Research Center of Pesticide and Medicine Intermediate Clean Production, Ministry of Education, Key Laboratory of Molecular and Nano Probes, Ministry of Education, Shandong Normal University, 88 East Wenhua Road, Jinan 250014, P. R. China. E-mail: tangb@sdnu.edu.cn; Fax: +86-531-86186033; Tel: +86-531-86182544

† CCDC reference numbers 675992 and 675993. For crystallographic data in CIF or other electronic format see DOI: 10.1039/b823360h

transition metal ions like Cd^{2+}, Fe^{2+}, Mn^{2+}, Ni^{2+}, Hg^{2+}, Co^{2+}, and Fe^{3+} (25 equivalent tolerance). Therefore, the probe could monitor intracellular Cu^{2+} levels with high selectivity and sensitivity in living cells. Besides, our probe could be easily synthesized through a two-step reaction of rhodamine 6 G with 2-acetyl-(1,4)-benzodiazine under mild conditions with a large throughput (~80%).

Results and discussion

Design strategy and synthesis of probe 2

Probe **2** was facilely synthesized from rhodamine 6 G by a two-step reaction. After column chromatography using CH_2Cl_2–CH_3OH (30 : 1, v/v), **2** was obtained in an 80% yield (Scheme 1).

A single crystal of **2** was grown from a CH_2Cl_2–CH_3OH (1 : 1, v/v) solution and was characterized using X-ray crystallography (Fig. 1). The crystal structure clearly represents the unique spirolactam-ring formation. Such a special conformation of the rhodamine group makes probe **2** colorless or fluorescence-inactive in solution. Therefore, probe **2** is expected to act as a signal switcher, which is envisioned to turn on when the target cation is bound.

Spectroscopic properties and optical responses to Cu^{2+}

Initially, we investigated the spectral properties of the probe under simulated physiological conditions (20 mM phosphate-buffered saline, PBS buffer, pH 7.4). The probe exhibited an emission maximum at 545 nm and the quantum yield was 0.062. The low quantum yield resulted from the spirolactam structure of the probe. Upon addition of Cu^{2+}, the fluorescence intensity increased in a Cu^{2+} concentration-dependent way and the quantum yield increased to 0.176 (Fig. 2), which can be ascribed to the delocalized xanthene moiety of the rhodamine group. Moreover, there was a good linear correlation (R = 0.9983) between relative fluorescent intensity and Cu^{2+} concentration in the range from 5.0×10^{-7} to 1.0×10^{-6} M. The regression equation was $F = 951.2[Cu^{2+}] + 2811.7$ (Fig. 3). The detection limit was 37 nM. This result showed that the probe could detect Cu^{2+} both qualitatively and quantitatively. Fig. 4, the Job plot analysis, revealed that the inflection point was at ~0.5, indicating that the probe forms a 1 : 1 species with Cu^{2+} in solution. According to the linear Benesi–Hildebrand expression,[56] the association constant (K_d) of the probe with Cu^{2+} ion in water was found to be 0.1 μM.

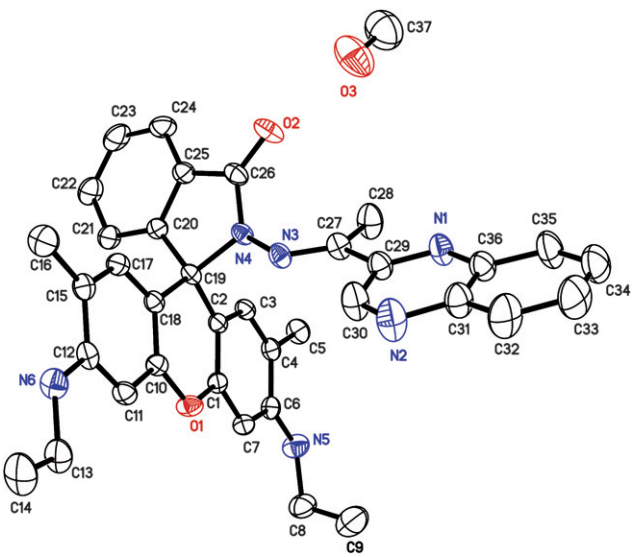

Fig. 1 X-Ray crystal structure of probe **2**, $C_{36}H_{34}N_6O_2 \cdot CH_3OH$. Displacement ellipsoids drawn at the 30% probability level.

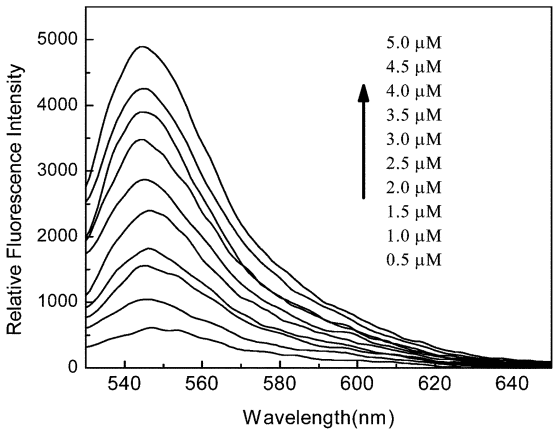

Fig. 2 Emission spectra (excitation at 520 nm) of 5.0 μM probe **2** in the presence of various concentrations of Cu^{2+} ranging from 0.50 to 5.0 μM. These spectra were measured in PBS buffer (20 mM, pH 7.4).

Reaction conditions

To determine the optimum reaction conditions for the analysis of Cu^{2+}, the effect of pH, buffer solution and the concentration of the fluorescent probe were investigated.

Effect of pH and buffer concentration. The effect of pH on the fluorescence of the probe was evaluated. PBS was used because it has been shown to be a better buffer for the incubation of mammalian cells, and may improve the planting efficiency of cell incubation and breed ability of cell. The relative fluorescence

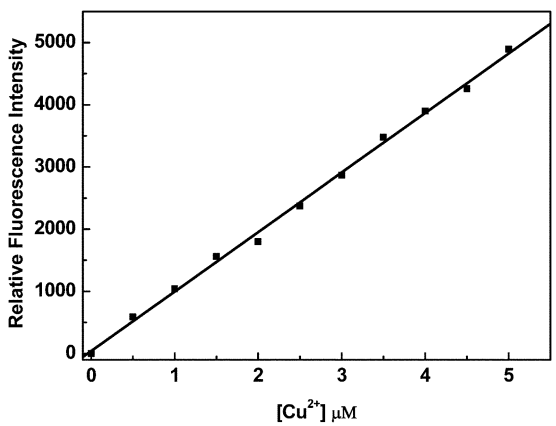

Fig. 3 Linear correlation between the relative fluorescence intensity and Cu^{2+} concentration. Probe **2** 5.0 μM in the presence of various concentrations of Cu^{2+} ranging from 0.50 to 5.0 μM.

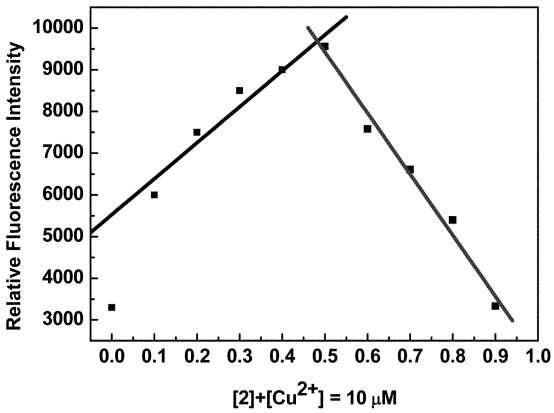

Fig. 4 Job plot: the relationship between probe [**2**] + [Cu^{2+}] and relative fluorescence intensity. The total concentration of probe **2** and Cu^{2+} was kept at a constant 10 μM. Excitation was provided at 520 nm and the emission intensity was measured at 545 nm. Spectra were acquired in 20 mM PBS buffer, pH 7.4. The data are consistent with a 1 : 1 (Cu^{2+} : probe **2**) complex.

intensity is not strongly dependent on pH from 6.2 to 7.8 (Fig. 5A). That is to say, the probe works well under physiological conditions. The buffer concentration also affects the fluorescence intensity. Fig. 5B shows that the relative fluorescence intensity of the system is stable at buffer concentrations of

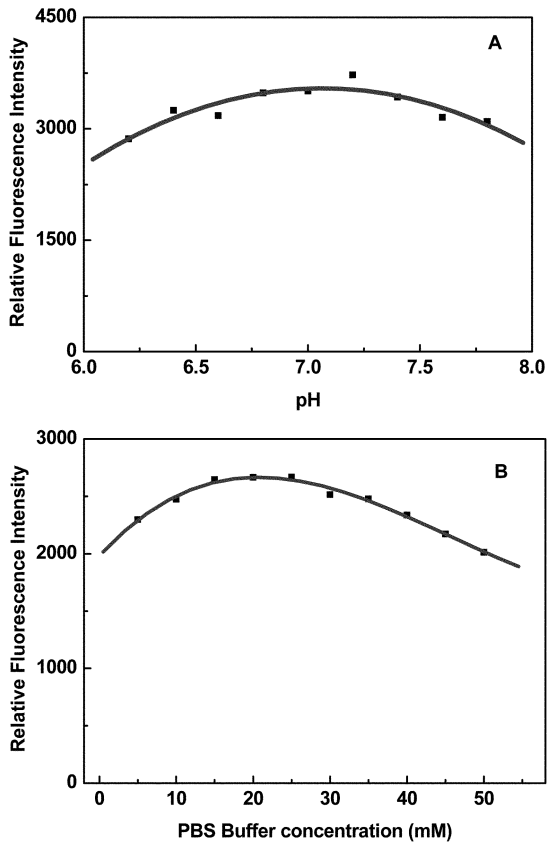

Fig. 5 (A) Effect of pH on the relative fluorescence intensity probe **2** (5.0 μm, PBS buffer 20 mM, pH 6.2–7.8), Cu^{2+} (1.0 μm). (B) Effect of buffer concentration (PBS, pH 7.40). The buffer concentration is from 5 to 50 mM.

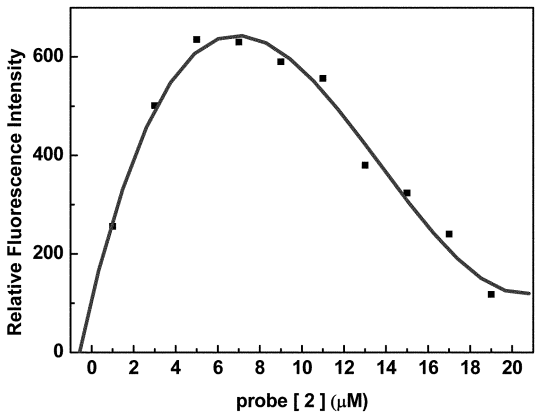

Fig. 6 Effect of the fluorescent probe concentration (probe **2**: 2.0–20.0 μM; Cu^{2+}: 5.0 μM, PBS buffer 20 mM, pH 7.4).

15–25 mM. Therefore, 20 mM of PBS (pH 7.40) is used throughout. In fact, a lower concentration of PBS has a poor buffer capacity, and superfluous PBS leads to a salt effect that decreases fluorescence intensity

Effect of the fluorescent probe concentration. The concentration of the probe directly decided whether Cu^{2+} was trapped completely, which determined the precision and sensitivity of the analytical method. The relative fluorescence intensity increased as the probe concentration increased (<5.0 μM), reached a plateau at the probe concentrations of 5.0–7.0 μM, and then decreased (Fig. 6). The result notes that a suitable concentration of the probe is important. Here, the 5.0 μM probe is chosen in this paper.

Test for probe selectivity

To assess the selectivity of the method, the interference of other metal ions on the determination of 1.0 μM Cu^{2+} was examined. An error of ±5.0% in the relative fluorescence intensity was considered tolerable. Fig. 7 displayed the fluorescence responses of a 5.0 μM concentration of **2** to the presence of various biologically relevant metal ions. The emission response of **2** was highly Cu^{2+}-selective. The emission had no evident changes in the presence of 1.0 mM Na^{+}, K^{+}, Ca^{2+}, Mg^{2+}, and Zn^{2+}. The result indicates excellent selectivity for Cu^{2+} over these abundant cellular cations. Other first-row transition metal ions, including 25 μM Cd^{2+}, Fe^{2+}, Mn^{2+}, Ni^{2+}, Hg^{2+}, Co^{2+}, and Fe^{3+}, produced no discernible changes in fluorescence intensities.

Kinetic assay

Fig. 8 shows the time course for the relative fluorescence intensity of the probe (5.0 μM, PBS buffer 20 mM, pH 7.4) treated with Cu^{2+} (1.0 μM) at room temperature. The experiment indicates that the reaction of the probe with Cu^{2+} can be instantly carried out under these conditions within 10 min, and that the probe solution is stable to the medium, light, and air.

Reversibility of Cu^{2+}-induced fluorescence

Fig. 9 displays the reversible binding of Cu^{2+} to probe **2** upon addition of the chelating agent *N*,*N*,*N*′,*N*′-tetrakis(2-picolyl) ethylenediamine (TPEN).

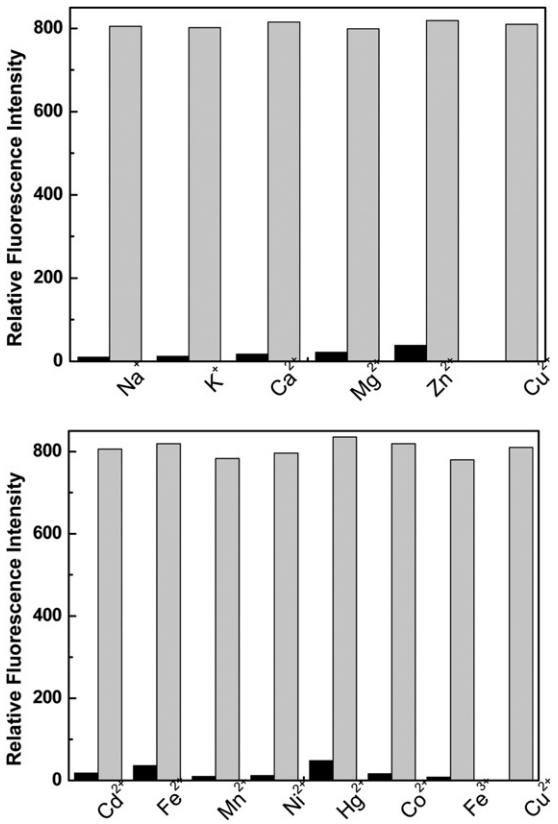

Fig. 7 Relative fluorescence intensity of probe **2** (5.0 μM) in the presence of various cations of interest. Black bars represent the addition of an excess of the appropriate metal ion (1.0 mM for Na^+, K^+, Ca^{2+}, Mg^{2+}, and Zn^{2+}, 25 μM for all other cations) to a 5.0 μM solution of probe **2**. Gray bars represent the subsequent addition of 1.0 μM Cu^{2+} to the solution. Excitation was provided at 520 nm.

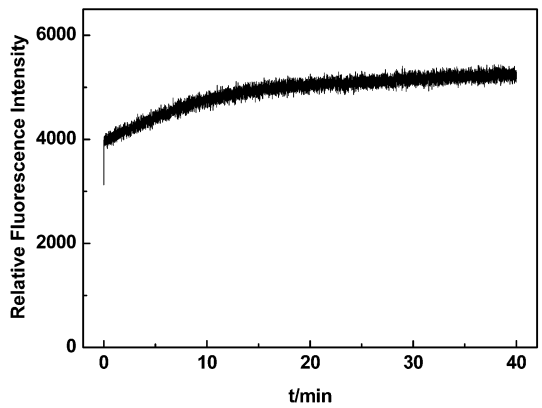

Fig. 8 Time course for the fluorescence response of probe **2** (5.0 μM, PBS buffer 20 mM, pH 7.4) to Cu^{2+} (1.0 μM) at room temperature.

Proposed mechanism for the reaction of 2 with Cu^{2+}

The proposed mechanism for the fluorescent probe is explained in Scheme 2. The mechanism of the probe is based on a change in structure between spirocyclic and open-cycle forms. Without Cu^{2+}, the probe exists in a spirocyclic form, which is colorless and non-fluorescent. As expected, addition of Cu^{2+} leads to

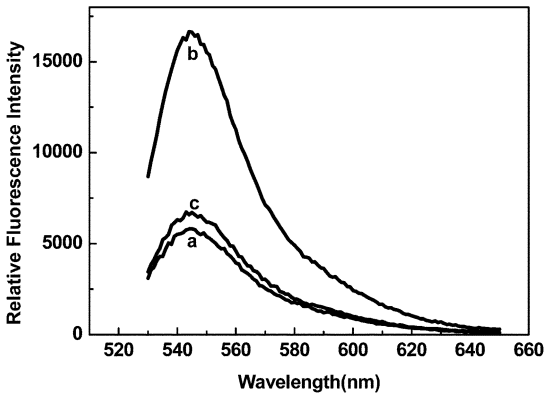

Fig. 9 Reversibility of Cu^{2+} binding to probe **2** upon addition of TPEN with excitation at 520 nm: (a) free probe **2**, [**2**] = 5.0 μM; (b) fluorescence increase upon addition of 1 equiv. Cu^{2+}; (c) decrease in fluorescence resulting from addition of 1 equiv. TPEN.

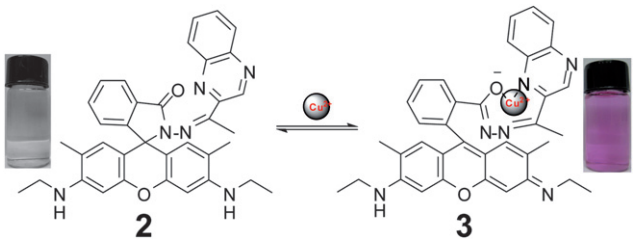

Scheme 2 Proposed mechanism for the fluorescence enhancement of **2** upon the addition of Cu^{2+}.

a spirocycle opening, resulting in an appearance of pink color and fluorescence (Scheme 2). There is significant enhancement of absorbance and fluorescence intensities in the 520–620 nm

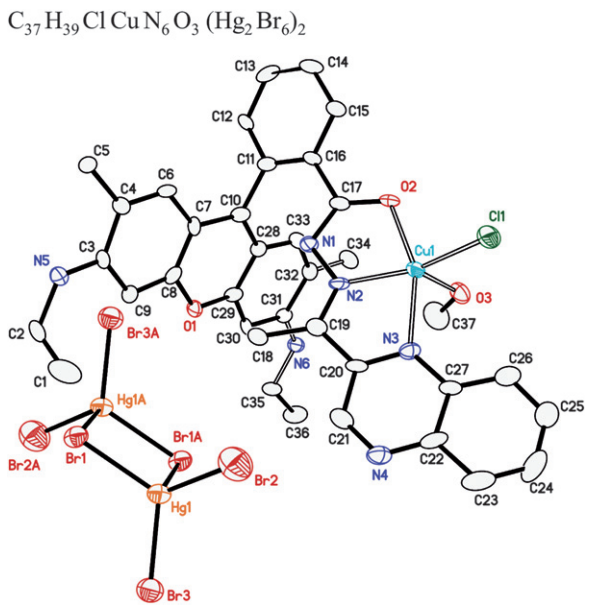

Fig. 10 X-Ray crystal structure of compound **3**. A: $(1 - x, 1 - y, 2 - z)$. Displacement ellipsoids drawn at the 50% probability level.

naked-eye probe selective for Cu(II) under physiological conditions.

Compound **3** was obtained by combination of compound **2** with $CuCl_2$ and $HgBr_2$ in a CH_2Cl_2/CH_3OH mixed-solvent system (metal : metal : ligand ratio = 2 : 2 : 1). As shown in Fig. 10, compound **3** crystallizes in the triclinic system $P\bar{1}$, and one kind of crystallographic Cu(II) center and two Hg(II) ions exist in compound **3**. It is noteworthy that the Cu(II) center lies in a $\{CuO_2N_2Cl\}$ coordination environment which consists of one quinoxaline N-donor (*d*Cu(1)–N(3) = 2.105(9) Å), one imine N-donor (*d*Cu(1)–N(2) = 1.928(11) Å), two O-donors from the acyl-O (*d*Cu(1)–O(2) = 2.013(8) Å) and methanol-O (*d*Cu(1)–O(3) = 2.203(10) Å), and one chlorine atom (*d*Cu(1)–Cl(1) = 2.216(4) Å). In addition, there are also two Hg(II) atoms which respectively reside in a distorted tetrahedral coordination sphere $\{HgBr_4\}$, where the $[Hg_2Br_6]$ moiety lies about an inversion center, and the Br–Hg bond lengths reveal greater and more obvious difference from 2.496(3) Å to 2.776(4) Å. Comparatively, the only Cu(II) coordination chemistry and the shorter length around the Cu(II) effectively demonstrate the strong interactions between the target ligand and Cu(II) atom, which also shows remarkably selectivity in fluorescence.

MTT assay

To evaluate the cytotoxicity of the probe and Cu^{2+}, we performed an MTT (3-(4,5-dimethylthiazol-2-yl)-2,5-diphenyltetrazolium bromide) assay in RAW264.7 cells with probe concentrations from 0.01 μM to 10.0 mM. The result showed IC_{50} = 110 μM (cells incubated with 5.0 μM Cu^{2+}, IC_{50} = 106 μM), which clearly demonstrated that the probe and 5.0 μM Cu^{2+} were of low toxicity to cultured cell lines under the experimental conditions at the operating concentration.

Confocal fluorescence imaging: Cu^{2+} detection in living cells

Levels of Cu^{2+} vary *in vivo*. In the brain, average neural intracellular copper concentrations are on the order of 0.1 mM.[4,57] However, copper is too redox-active to exist in an unbound form in the cell without causing oxidative damage, and an upper limit of the free concentration of Cu(II) in unstressed cells has been evaluated to be 10^{-18} M.[1,58] Therefore, Cu^{2+} ion is bound by small anions, polypeptides, enzymes, and proteins, with an affinity in the range between 1 nM and 10 μM or even in the femtomolar range.[1,59] It must be pointed out that the affinity with enzymes and proteins is mostly lower than 0.1 μM, which makes it possible for detecting intracellular Cu^{2+} concentration in the labile copper pool with our probe **2**, because the copper ion can reach ≥100 μM in some pathological cells.[1,4,57–60]

Finally, we applied the probe in RAW264.7 macrophages to examine whether it worked in biological systems. As determined by laser scanning confocal microscopy, staining RAW264.7 cells with 5.0 μM probe for 30 min at 37 °C gave nearly no intracellular fluorescence (Fig. 11a). When the cells were supplemented with 5.0 μM Cu^{2+} in the growth medium for 30 min at 37 °C and then incubated with probe under the same conditions, a significant fluorescence increase from the intracellular region was observed (Fig. 11c). Bright-field measurements after treatment with Cu^{2+} and probe confirmed that the cells were viable throughout the imaging experiments (Fig. 11b and 11d). The overlay of fluorescence and bright-field images revealed that the fluorescence signals were localized in the perinuclear region of the cytosol (Fig. 11e), indicating the subcellular distribution of Cu^{2+} which was internalized into the living cells from the growth medium. The results of fluorescence microscopic analyses of treated cells show that the probe can be used for monitoring Cu^{2+} within biological samples.

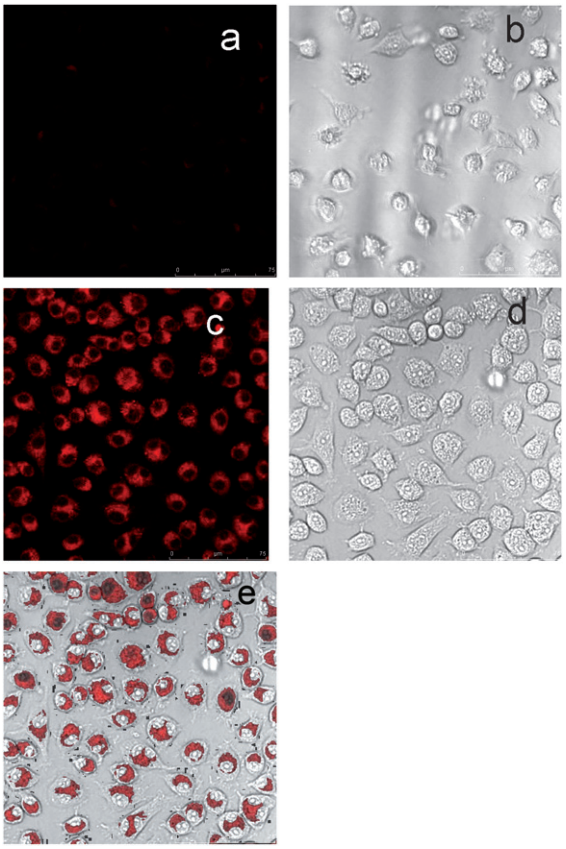

Fig. 11 Confocal fluorescence images of living RAW264.7 macrophages, bar is 75 μm. (a) Cells incubated with 5.0 μM probe **2** for 30 min at 37 °C; (b) bright-field of panel (a). (c) Cells with 5.0 μM Cu^{2+} added to the dye-loaded RAW264.7 macrophages. The cells were incubated with Cu^{2+} for 30 min at 37 °C; (d) bright-field image of live RAW264.7 macrophages shown in panel (c), confirming their viability. (e) Overlay image of (c) and (d).

Experimental

Materials

Rhodamine 6 G was purchased from Sigma-Aldrich Co. All other reagents and solvents were purchased from commercial sources and of the highest grade. Silica gel (200–300 mesh, Qingdao Haiyang Chemical Co.) was used for column chromatography. Analytical thin-layer chromatography was performed using GF254 silica gel (precoated sheets, 0.77 mm thick, Taizhou Si-Jia Biochemical Plastic Company). RAW264.7 cells were purchased from American Type Culture Collection, Manassas, VA, USA.

Apparatus

^{1}H-NMR spectra were recorded on Bruker Avance 300 MHz apparatus. Fluorimetric spectra and traces were obtained with an Edinburgh FLS920 spectrofluorimeter (Edinburgh Instruments Ltd, UK) equipped with a xenon lamp and 1.0 cm quartz cells. X-Ray intensity data were measured on a Bruker SMART APEX CCD-based diffractometer (Mo Kα radiation, $\lambda = 0.71073$ Å). The pH measurements were performed on a pHS-3C digital pH-meter (LeiCi, Shanghai, China) with a combined glass–calomel electrode. Ultrapure water was used throughout. The images were taken using an LTE confocal laser scanning microscope (Germany Leica Co., Ltd) with an objective lens (×40). The excitation wavelength was 532 nm.

Crystal data text

Crystal data for **2**: $C_{37}H_{38}N_6O_3$; triclinic; $P\bar{1}$; $M_r = 614.73$; $a = 10.023(3)$, $b = 12.111(3)$, $c = 15.207(4)$ Å; $\alpha = 71.030(2)$, $\beta = 77.030(2)$, $\gamma = 79.031(2)°$; $V = 1608.5(7)$ Å^3; $Z = 2$, $\rho_{calcd} = 1.269$ mg m^{-3}; μ(Mo Kα) = 0.083 mm^{-1}; $F(000) = 652$; $T = 298(2)$ K; λ(Mo Kα) = 0.71073 Å; $\theta_{max} = 25.01°$; reflections collected/unique: 8183/5583 ($R_{int} = 0.0195$); R_1 ($I > 2\sigma(I)$) = 0.0666; wR_2 ($I > 2\sigma(I)$) = 0.1713.†

Crystal data for **3**: $C_{37}H_{39}Br_3ClCuHgN_6O_3$; triclinic; $P\bar{1}$; $M_r = 1155.05$; $a = 9.5212(16)$, $b = 11.861(2)$, $c = 17.621(3)$Å; $\alpha = 92.939(3)$, $\beta = 94.128(3)$, $\gamma = 102.065(2)°$; $V = 1936.5(6)$ Å^3; $Z = 2$, $\rho_{calcd} = 1.981$ mg m^{-3}; μ(Mo Kα) = 7.717 mm^{-1}; $F(000) = 1116$; $T = 173(2)$ K; λ(Mo Kα) = 0.71073 Å; $\theta_{max} = 25.50°$; reflections collected/unique: 10218/7079 ($R_{int} = 0.0356$); R_1 ($I > 2\sigma(I)$) = 0.0671; wR_2 ($I > 2\sigma(I)$) = 0.1769.†

3-(4,5-Dimethylthiazol-2-yl)-2,5-diphenyltetrazolium bromide (MTT) assay

RAW264.7 cells (10^6 cellsg mL^{-1}) were dispersed within replicate 96-well microtiter plates to a total volume of 200 μL well^{-1}. Plates were maintained at 37 °C in a 5% CO_2/95% air incubator for 4 h. RAW264.7 cells were then incubated for 24 h upon different concentrations probe of 10^{-3}, 10^{-4}, 10^{-5}, 10^{-6}, 10^{-7} and 10^{-8} M respectively. MTT (Sigma) solution (5.0 mg mL^{-1}, HEPES) was then added to each well. After 4 h, the remaining MTT solution was removed, and 150 μL of DMSO was added to each well to dissolve the formazan crystals. Absorbance was measured at 490 nm in a TRITURUS microplate reader. Calculation of IC_{50} values was done according to Huber and Koella.[61] The same operation was perfomed with the cells that had been incubated with 5.0 μM Cu^{2+}.

Synthesis

Preparation of 1. Rhodamine 6 G hydrazide was prepared according to a literature method.[62] Rhodamine 6 G (1.916 g, 4.0 mmol) was dissolved in 60 mL ethanol. 6.0 mL (excess) hydrazine monohydrate (85%) was then added dropwise with vigorous stirring at room temperature. After the addition, the stirred mixture was heated to reflux for 3 h, during which the dark purple solution disappeared and pink precipitate appeared after cooling overnight. The resulting precipitate was filtered and washed three times with 20 mL CH_3CH_2OH–H_2O (1 : 1, v/v). After drying in vacuum, the reaction afforded rhodamine 6 G hydrazide **1** (1.45 g, yield: 85%). ^{1}H-NMR (DMSO), δ (ppm): 1.20 (6H), 1.86 (6H), 3.12 (4H), 4.20 (2H), 4.97 (2H), 6.09 (2H), 6.26 (2H), 6.93 (1H), 7.46 (2H), 7.78 (1H).

Preparation 2. Rhodamine 6 G hydrazide (2.0 mmol, 0.956 g) and 2-acetyl-(1, 4)-benzodiazine (2.0 mmol, 0.344 g) were mixed in boiling methanol after adding 0.10 mL acetic acid and refluxed for 3 h. A light yellow precipitate obtained was filtered off, washed with methanol–diethyl ether (1 : 1, v/v) and dried in vacuum. The crude product was purified by column chromatography (CH_2Cl_2–CH_3OH = 30 : 1, v/v). Yield: 1.04 g, 80%. ^{1}H-NMR (DMSO) δ (ppm): 1.20 (6H), 1.89 (6H), 2.40 (3H), 3.12 (4H), 5.03 (2H), 6.28 (4H), 7.16 (1H), 7.63 (2H), 7.89 (3H), 8.07 (2H), 8.96 (1H); ^{13}C-NMR (DMSO) δ (ppm): 14.75, 38.08, 17.56, 67.62, 96.19, 97.48, 102.79, 106.12, 118.65, 123.69, 124.62, 127.92, 129.43, 130.06, 130.47, 131.42, 131.72, 133.91, 141.06, 142.27, 143.62, 148.24, 149.47, 151.77, 152.05, 160.29, 166.85.

Sample preparation

The probe was dissolved in CH_3CN as a stock solution (0.10 mM). Aqueous metal ions solutions of Zn^{2+}, Hg^{2+}, Co^{2+}, Ni^{2+}, Cd^{2+} and Mn^{2+} were prepared from the acetates. Solutions of Na^+, K^+, Ca^{2+}, Fe^{3+} and Mg^{2+} were prepared from chlorides. The Fe^{2+} solution was prepared immediately before use with ferrous ammonium sulfate.

Fluorescence analysis

Fluorescence emission spectra were obtained with a Xenon lamp and 1.0 cm quartz cells. Different concentrations of Cu^{2+} were added to PBS buffer (2.0 mL, 0.10 M) and probe 2 (0.50 mL, 0.10 mM) in 10 mL color comparison tube. After dilution with ultrapure water, the mixture was equilibrated for 10 min before measurement. The fluorescence intensity was measured simultaneously at $\lambda_{ex/em}$ = 520/545 nm. The excitation and emission slits were set to 1.0 nm and 1.5 nm, respectively.

Cell incubation and imaging

RAW264.7 macrophages were cultured in Dulbecco's modified Eagle's medium containing 10% fetal bovine serum, 1% penicillin, and 1% streptomycin at 37 °C in a 5% CO_2/95% air incubator MCO-15AC (SANYO). The concentration of counted cells was adjusted to 1.0×10^6 cells mL^{-1} and cells were passed and plated on glass slide at 37 °C, 5% CO_2 for 4 h. Some of adherent cells were incubated with 5.0 μM probe **2** for 0.5 h at 37 °C under 5% CO_2 and then washed with PBS three times before incubating with 5.0 μM $CuCl_2$ for another 0.5 h, cells were rinsed with PBS three times again, then the fluorescence imaging of intracellular Cu^{2+} was observed under a LSM510 confocal laser scanning microscope (Zeiss) with an objective lens (×40). The RAW264.7 macrophages only incubated with 5.0 μM **2** for 0.5 hour at 37 °C under 5% CO_2 was as a control.

Conclusions

In conclusion, we have described the synthesis, properties and cellular applications of probe **2** which is a new fluorescent probe

to monitor intracellular Cu^{2+} levels in living cells. The new fluorescent probe displays highly selective for Cu^{2+} over than other metal ions under physiological conditions. Both fluorescent also facilitate naked-eye detection of Cu^{2+}. Furthermore, we have demonstrated the application in biology by imaging intracellular Cu^{2+} in RAW264.7 macrophages. We believe that the highly sensitive and selective fluorescent probe will have great potential in investigating the pivotal role of copper in biological systems.

Acknowledgements

This work was supported by National Basic Research Program of China (973 Program, 2007CB936000), National Natural Science Funds for Distinguished Young Scholar (No. 20725518), Major Program of National Natural Science Foundation of China (No. 90713019), National Natural Science Foundation of China (No. 20575036) Important Project of Natural Science Foundation of Shandong Province in China (No. Z2006B09) and the Research Foundation for the Doctoral Program of Ministry of Education (No. 20060445002).

References

1 E. Gaggelli, H. Kozlowski, D. Valensin and G. Valensin, *Chem. Rev.*, 2006, **106**, 1995–2044.
2 *Handbook of metalloproteins*, ed. A. Messerschmidt, R. Huber, T. Poulos and K. Weighardt, John Wiley & Sons, Chichester, 2001, vol. 2, pp. 1149–1413.
3 S. Hu, P. Furst and D. Hamer, *New Biol.*, 1990, **2**, 544–555.
4 E. L. Que, D. W. Domaille and C. J. Chang, *Chem. Rev.*, 2008, **108**, 4328–4359.
5 D. J. Waggoner, T. B. Bartnikas and J. D. Gitlin, *Neurobiol. Disease*, 1999, **6**, 221–230.
6 C. Vulpe, B. Levinson, S. Whitney, S. Packman and J. Gitschier, *Nat. Genet.*, 1993, **3**, 7–13.
7 P. C. Bull, G. R. Thomas, J. M. Rommens, J. R. Forbes and D. W. Cox, *Nat. Genet.*, 1993, **5**, 327–337.
8 J. S. Valentine and P. J. Hart, *Proc. Natl. Acad. Sci. U. S. A.*, 2003, **100**, 3617–3622.
9 L. I. Bruijn, T. M. Miller and D. W. Cleveland, *Annu. Rev. Neurosci.*, 2004, **27**, 723–749.
10 K. J. Barnham, C. L. Masters and A. I. Bush, *Nat. Rev. Drug Discovery*, 2004, **3**, 205–214.
11 D. R. Brown and H. Kozlowski, *Dalton Trans.*, 2004, 1907–1917.
12 (*a*) G. Muthaup, A. Schlicksupp, L. Hess, D. Beher, T. Ruppert, C. L. Masters and K. Beyreuther, *Science*, 1996, **271**, 1406–1409; (*b*) R. A. Løvstad, *BioMetals*, 2004, **17**, 111–113.
13 B. Tang, L. J. Cui, K. H. Xu, L. L. Tong, G. W. Yang and L. G. An, *ChemBioChem*, 2008, **9**, 1159–1164.
14 S. C. Burdette, G. K. Walkup, B. Spingler, R. Y. Tsien and S. J. Lippard, *J. Am. Chem. Soc.*, 2001, **123**, 7831–7841.
15 S. Yoon, A. E. Albers, A. P. Wong and C. J. Chang, *J. Am. Chem. Soc.*, 2005, **127**, 16030–16031.
16 L. Yang, R. McRae, M. M. Henary, R. Patel, B. Lai, S. Vogt and C. J. Fahrni, *Proc. Natl. Acad. Sci. U. S. A.*, 2005, **102**, 11179–11184.
17 Q. He, E. W. Miller, A. P. Wong and C. J. Chang, *J. Am. Chem. Soc.*, 2006, **128**, 9316–9317.
18 L. Zeng, E. W. Miller, A. Pralle, E. Y. Isacoff and C. J. Chang, *J. Am. Chem. Soc.*, 2006, **128**, 10–11.
19 S. V. Wegner, A. Okesli, P. Chen and C. He, *J. Am. Chem. Soc.*, 2007, **129**, 3474–3475.
20 E. M. Nolan and S. J. Lippard, *J. Am. Chem. Soc.*, 2007, **129**, 5910–5918.
21 B. Tang, H. Huang, K. H. Xu, L. L. Tong, G. W. Yang, X. Liu and L. G. An, *Chem. Commun.*, 2006, 3609–3611.
22 L. Fabrizzi, M. Licchelli, P. Pallavicini, A. Perotti and D. Sacchi, *Angew. Chem., Int. Ed. Engl.*, 1994, **33**, 1975–1977.
23 A. Torrado, G. K. Walkup and B. Imperiali, *J. Am. Chem. Soc.*, 1998, **120**, 609–610.
24 Y. Zheng, K. M. Gatta's-Asfura, V. Konka and R. M. Leblanc, *Chem. Commun.*, 2002, 2350–2351.
25 Y. Zheng, X. Cao, J. Orbulescu, V. Konka, F. M. Andreopoulos, S. M. Pham and R. M. Leblanc, *Anal. Chem.*, 2003, **75**, 1706–1712.
26 P. Grandini, F. Mancin, P. Tecilla, P. Scrimin and U. Tonellato, *Angew. Chem., Int. Ed.*, 1999, **38**, 3061–3064.
27 A. Mokhir, A. Kiel, D. P. Herten and R. Kraemer, *Inorg. Chem.*, 2005, **44**, 5661–5666.
28 Y. J. Mei, P. A. Bentley and W. Wang, *Tetrahedron Lett.*, 2006, **47**, 2447–2449.
29 P. Comba, R. Kramer, A. Mokhir, K. Naing and E. Schatz, *Eur. J. Inorg. Chem.*, 2006, 4442–4448.
30 J. K. Choi, S. H. Kim, J. Yoon, K. H. Lee, R. A. Bartsch and J. S. Kim, *J. Org. Chem.*, 2006, **71**, 8011–8015.
31 S. M. Park, M. H. Kim, J. I. Choe, K. T. No and S. K. Chang, *J. Org. Chem.*, 2007, **72**, 3550–3553.
32 J. Xie, M. Me'nand, S. Maisonneuve and R. Me'tivier, *J. Org. Chem.*, 2007, **72**, 5980–5985.
33 Y. Q. Wen, F. Yue, Y. R. Zhong and B. H. Ye, *Inorg. Chem.*, 2007, **46**, 7749–7755.
34 A. W. Varnes, R. B. Dodson and E. L. Wehry, *J. Am. Chem. Soc.*, 1972, **94**, 946–950.
35 J. A. Kemlo and T. M. Shepherd, *Chem. Phys. Lett.*, 1977, **47**, 158–162.
36 V. Dujols, F. Ford and A. W. Czarnik, *J. Am. Chem. Soc.*, 1997, **119**, 7386.
37 J. S. Yang, C. S. Lin and C. Y. Hwang, *Org. Lett.*, 2001, **3**, 889–892.
38 S. Kaur and S. Kumar, *Chem. Commun.*, 2002, 2840–2841.
39 Q. Wu and E. V. Anslyn, *J. Am. Chem. Soc.*, 2004, **126**, 14682–14683.
40 M. Royzen, Z. Dai and J. W. Canary, *J. Am. Chem. Soc.*, 2005, **127**, 1612–1613.
41 Z. Xu, Y. Xiao, X. Qian, J. Cui and D. Cui, *Org. Lett.*, 2005, **7**, 889–892.
42 Z. C. Wen, R. Yang, H. He and Y. B. Jiang, *Chem. Commun.*, 2006, 106–108.
43 H. Yang, Z. Q. Liu, Z. G. Zhou, E. X. Shi, F. Y. Li, Y. K. Du, T. Yi and C. H. Huang, *Tetrahedron Lett.*, 2006, **47**, 2911–2914.
44 R. Martinez, F. Zapata and A. Caballero, *Org. Lett.*, 2006, **8**, 3235–3238.
45 J. Liu and Y. Lu, *J. Am. Chem. Soc.*, 2007, **129**, 9838–9839.
46 K. M. K. Swamy, S.-K. Ko, S. K. Kwon, H. N. Lee, C. Mao, J.-M. Kim, K.-H. Lee, J. K., I. Shin and J. Yoon, *Chem. Commun.*, 2008, 5915–5917.
47 J. Y. Kwon, Y. J. Jang, Y. J. Lee, K. M. Kim, M. S. Seo, W. Nam and J. Yoon, *J. Am. Chem. Soc.*, 2005, **127**, 10107–10111.
48 M. H. Lee, J. S. Wu, J. W. Lee, J. H. Jung and J. S. Kim, *Org. Lett.*, 2007, **9**, 2501–2504.
49 J. S. Wu, I. C. Hwang, K. S. Kim and J. S. Kim, *Org. Lett.*, 2007, **9**, 907–910.
50 H. Zheng, Z. H. Qian, L. Xu, F. F. Yuan, L. D. Lan and J. G. Xu, *Org. Lett.*, 2006, **8**, 859–861.
51 D. Wu, W. Huang, C. Y. Duan, Z. H. Lin and Q. J. Meng, *Inorg. Chem.*, 2007, **46**, 1538–1540.
52 Y. K. Yang, K. J. Yook and J. Tae, *J. Am. Chem. Soc.*, 2005, **127**, 16760–16761.
53 S. K. Ko, Y. K. Yang, J. Tae and I. Shin, *J. Am. Chem. Soc.*, 2006, **128**, 14150–14155.
54 Y. Xiang and A. Tong, *Org. Lett.*, 2006, **8**, 1549–1552.
55 X. Zhang, Y. Shiraishi and T. Hirai, *Org. Lett.*, 2007, **9**, 5039–5042.
56 (*a*) H. A. Benesi and J. H. Hildebrand, *J. Am. Chem. Soc.*, 1949, **71**, 2703–2707; (*b*) M. Barra, C. Bohne and J. C. Scaiano, *J. Am. Chem. Soc.*, 1990, **112**, 8075–8579.
57 J. Stöckel, J. Safar, A. C. Wallace, F. E. Cohen and S. B. Prusiner, *Biochemistry*, 1998, **37**, 71857193.
58 (*a*) T. D. Rae, P. J. Schmidt, R. A. Pufahl, V. C. Culotta and T. V. O'Halloran, *Science*, 1999, **284**, 805–808; (*b*) S. J. Lippard, *Science*, 1999, **284**, 748–749.
59 (*a*) C. S. Burns, E. Aronoff-Spencer, G. Legname, S. B. Prusiner, W. E. Antholine, G. J. Gerfen, J. Peisach and G. L. Millhauser, *Biochemistry*, 2003, **42**, 6794–6803; (*b*) R. M. Whittal, H. L. Ball, F. E. Cohen, A. L. Burlingame, S. B. Prusiner and M. A. Baldwin,

Protein Sci., 2000, **9**, 332–343; (*c*) G. S. Jackson, I. Murray, L. L. Hosszu, N. Gibbs, J. P. Waltho, A. R. Clarke and J. Collinge, *Proc. Natl. Acad. Sci. U. S. A.*, 2001, **98**, 8531–8535; (*d*) M. L. Kramer, H. D. Kratzin, B. Schmidt, A. Romer, O. Windl, S. Liemann, S. Hornemann and H. J. Kretzschmar, *Biol. Chem.*, 2001, **276**, 16711–16719; (*e*) A. P. Garnett and J. H. Viles, *J. Biol. Chem.*, 2003, **278**, 6795–6802.

60 (*a*) P. C. Pauly and D. A. Harris, *J. Biol. Chem.*, 1998, **273**, 33107–33110; (*b*) W. Sumudhu, S. Perera and N. M. Hooper, *Curr. Biol.*, 2001, **11**, 519–523; (*c*) L. R. Brown and D. A. Harris, *J. Neurochem.*, 2003, **87**, 353–363.

61 W. Huber and J. C. Koella, *Acta Trop.*, 1993, **55**, 257–261.

62 X. F. Yang, X. Q. Guo and Y. B. Zhao, *Talanta*, 2002, **57**, 883–890.